RAPID COMMUNICATIONS

PHYSICAL REVIEW A VOLUME 57, NUMBER 3 MARCH 1998

Direct observation of atomic localization in optical superlattices

L. Guidoni and P. Verkerk
Laboratoire Kastler Brossel, Département de Physique de l'Ecole Normale Supérieure, 24 rue Lhomond, 75231 Paris Cedex 05, France
(Received 21 July 1997; revised manuscript received 29 September 1997)

We present direct experimental evidence for the localization of atoms cooled and trapped in a three-dimensional optical superlattice. As in the case of solid-state superlattices, we are able to tailor the characteristics of the optical potential wells. In particular, we impose a long-range modulation to the depth of the potential wells whose size remains in the optical wavelength range. The cooling mechanism in this configuration accumulates the atoms in the deepest wells. Images of the resulting separated denser atomic planes (distance $\simeq 70\ \mu$m) have been obtained both by detecting the fluorescence and by observing the shadow of the cloud. [S1050-2947(98)50204-1]

PACS number(s): 32.80.Pj, 68.65.+g

These past few years have seen a rapid development of the study of atoms trapped in optical lattices [1]. Such systems offer a close analogy with solid-state physics as atoms evolve in a periodic optical potential like the electrons in an ion matrix. The optical lattice has neither defects nor impurities because it is due to an interference pattern of several laser beams. Therefore, the atomic dynamics is unaffected by phononlike phenomena that can limit the coherence time. These properties allow us to test some subtle effects, such as Bloch oscillations, long predicted for solids [2] and recently observed in an optical lattice [3]. However, the periodic arrangement of atoms in the optical potential wells is only deduced from indirect experimental observations. The oscillation of the atoms at the bottom of the wells has been observed, detecting Raman transitions between vibrational levels, both by pump-probe spectroscopy [4] and by heterodyne analysis of the fluorescence [5]. Bragg scattering of light by optical lattices has demonstrated the long-range periodic order [6,7]. Direct observation of the periodic structure of optical lattices is not possible by imaging the fluorescence because the distance between adjacent sites is too small (of the order of the wavelength of the trapping beams). More recently, optical lattices have been extended to the quasiperiodic case [8,9], in close analogy with the field of quasicrystals [10]. Quasiperiodic optical lattices are obtained by adding extra beams to a standard four-beam lattice [11], so as to introduce at least two incommensurate periods. Taking this idea somewhat further, we describe here an experiment where the extra period is so large that we are able to resolve the fluorescence of the atoms trapped in the successive planes of this optical superlattice [12].

The arrangement of the trapping beams is depicted in Fig. 1. The underlying four-beam periodic lattice (darker arrows) consists of three beams in the horizontal xOy plane and a fourth beam that is vertical along Oz. The vertical period of the resulting four-beam optical potential is exactly imposed by the wavelength of the trapping beams. A fifth beam (lighter arrow in Fig. 1) lies in the xOz plane, vertically above one of the horizontal beams. For reasonably small angles (typically $1 < \Theta < 50$ mrad) a sinusoidal superperiodic modulation of the optical potential depth is imposed on the original four-beam periodic lattice. The spatial superperiod can be tuned between a few tens and a few hundreds of atomic planes just by choosing the angle Θ. This situation is then very similar to the case of superlattices in solid-state physics, where the electrons move in a periodic potential whose characteristics change from one layer to the next one [13].

The experiment is performed with cesium atoms that are first gathered and cooled in a low vapor pressure cell by the well-known magneto-optical trap (MOT) [14]. The six trapping beams and the inhomogeneous magnetic field are then switched off and we switch on a five-beam superlattice. Each of the beams has the same intensity, ranging from $I \simeq 0.1$ to 10 mW/cm^2 and the same frequency, detuned on the red side of the D_2 $F=4 \rightarrow F'=5$ transition of cesium (at 852.1 nm) by $\Delta/2\pi = -100$ MHz. The angle Θ between the two beams is 12.5 ± 0.8 mrad. The vertical period of the underlying lattice is $\lambda = 0.852\ \mu$m and the almost-vertical superperiod that arises is $\Lambda = \lambda/\Theta = 68 \pm 4\ \mu$m. The superlattice that we obtain is thus composed of potential wells, the depths of which are modulated on a scale of 80 atomic planes. The beam configuration of Fig. 1 leads to an unbalanced radiation pressure that tends to push the atoms upwards. However, when the detuning is sufficiently large, the radiation pressure force is much smaller than the dipole force [15]. In our experimen-

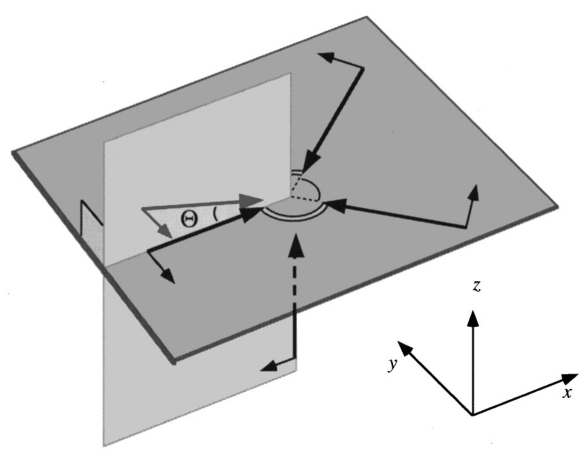

FIG. 1. Beam configuration used to create a superperiodic optical lattice. In the experiment, the angle Θ between the supplementary beam and the horizontal plane is $\Theta = 12.5 \pm 0.8$ mrad. Note that all the beam polarizations are parallel to the horizontal plane.

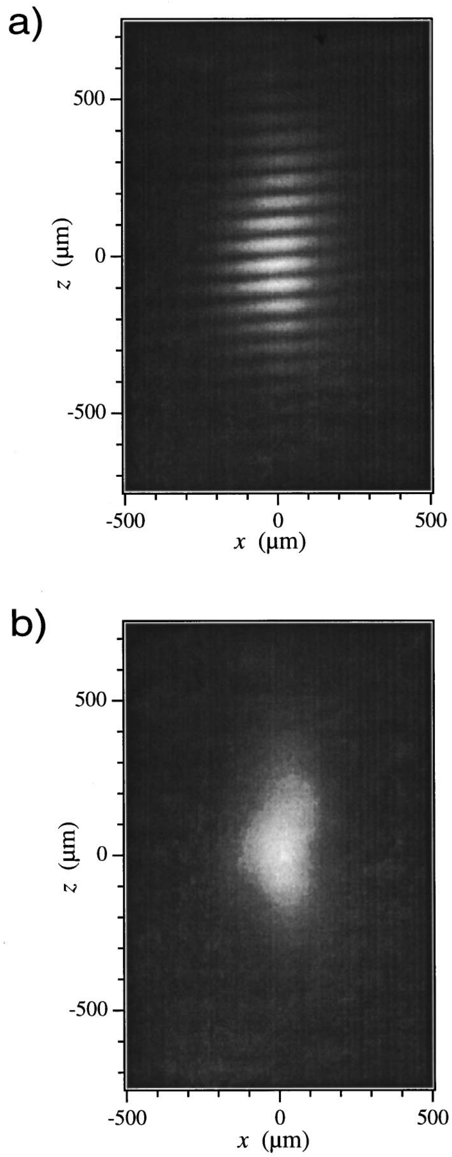

FIG. 2. (a) Image of the fluorescence emitted by a superperiodic optical lattice. The image is recorded by a 16-bit Peltier-cooled CCD camera with an exposure time of 10 ms. (b) Image of fluorescence obtained when the supplementary beam of the superlattice is blocked ($I_5=0$).

tal conditions, the cloud moves with an average velocity of about 1 mm/s and the lattice is observable for more than 500 ms.

In a first set of experiments, we have recorded the fluorescence of the atoms trapped in this superlattice. We observe the cloud from the *y* direction with a Peltier-cooled 16-bit charge-coupled-device (CCD) camera. The imaging system is composed of one meniscus lens followed by two doublets facing one another. The overall magnification is 2.5 and the theoretical ultimate resolution 7 μm, evaluated for a 50% modulation transfer function [16]. The pixels of the CCD camera are 22 μm $\times$ 22 μm wide. With this pixel dimension, we are not limited by the resolution of the imaging lenses. We record the fluorescence light with an exposure time of 10 ms. The resulting images taken for a lattice beam intensity of 4 mW/cm^2 are shown in Fig. 2. In particular, Fig. 2(a) shows the superlattice, while Fig. 2(b) shows the usual lattice obtained by blocking the fifth beam. The global shape of the cloud is the same, but the superlattice exhibits an intensity modulation, as expected.

It is important here to discuss the crucial differences between our experiment and the previously reported observations of striations in samples of laser-cooled atoms. The very first observation of spatially modulated fluorescence of cold atoms was reported in 1990 [17]. The system considered at that time was a MOT with a slight misalignment of the beams. As pointed out by Steane *et al.* [18], in that system the atomic localization is the result of a complex interplay of friction and dipole forces. An accurate description of the physical mechanisms involved is very difficult to obtain because it depends on the relative phases between the six trapping beams. Another very interesting system based on the rectified dipole force due to a bichromatic field has been studied by Grove *et al.* [19]. In that case the fluorescence of a pure one-dimensional lattice with a large spatial period (71 μm) was observed. Such a large spatial period was imposed by the beating between the two components of the bichromatic field. In order to localize the atoms in such a frictionless structure, rapidly alternated phases of magneto-optical trapping and rectified optical potential were necessary. An analogous system in two dimensions (2D) has been studied recently: a hologram generates a 2D array of far-detuned dipole traps and an additional gray molasses provides the friction mechanism [20]. By contrast, the situation we present here does not need any additional friction force and is perfectly described in terms of Sisyphus cooling, as in the case of a usual bright lattice. The superlattice that we obtain has two different length scales: the potential wells have an almost constant size imposed by λ, and their depths are modulated at λ/Θ scale. In spite of the presence of intermediate local minima, the atoms fill the deepest potential wells. Moreover, our structure is a three-dimensional optical lattice and then displays a lifetime of the order of the second. Therefore stable and low-noise images of the atomic sample can be easily obtained.

The observation of a modulated fluorescence does not prove the presence of a density modulation when the total intensity impinging on the atoms is itself spatially modulated. Even in the case of a uniform atomic distribution, a slight modulation should be observed in the fluorescent light. In order to confirm the presence of a density modulation, we therefore take the shadow image of the cloud in a resonant flash beam [21]. This flash beam is collimated and much wider than the atomic cloud. It is sent through the cloud onto the camera, using the previous imaging system. The flash is turned on for 100 μs during the 10-ms exposure time of the camera, just after the five beams of the superlattice have been switched off. Note that with this temporal sequence for the measurement, the images are not contaminated by the fluorescence of the lattice, and we probe completely free atoms, as in the Bragg scattering experiment of Ref. [6]. The flash intensity is 100 μW/cm^2, low enough that it saturates neither the atoms nor the camera. To extract the shadow image of the sample, we take two successive images with and without atoms by turning on and off the MOT. The resulting difference image is shown in Fig. 3(a). An averaged vertical profile of this image [see Fig. 3(b)] exhibits an uncorrected absorption modulation of approximately 30%.

RAPID COMMUNICATIONS

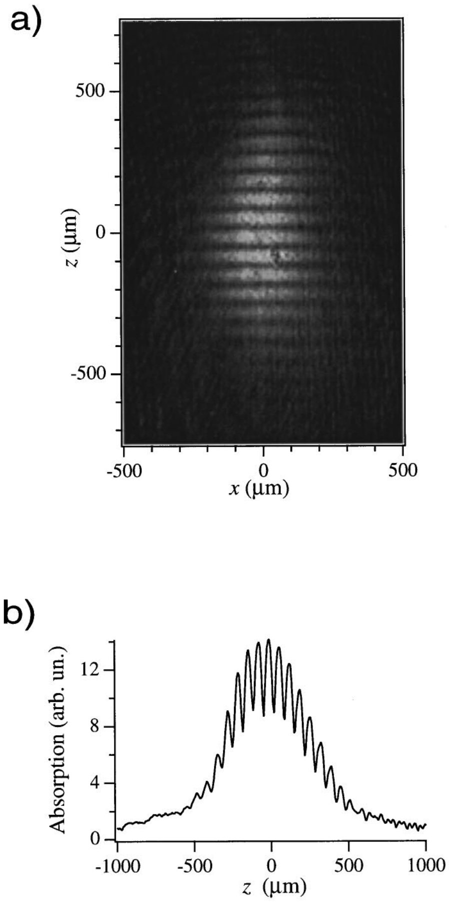

FIG. 3. (a) Shadow image of a superperiodic optical lattice obtained by using a weak, collimated, resonant beam. A first image is recorded after the lattice beams are switched off and and a second one is obtained when no trapped atoms are present. The resulting displayed image is obtained by substraction. (b) Vertical profile of the image in (a) averaged over ten horizontal pixels. The fitted density modulation is approximately 30%.

Note that, in an ideal shadow experiment, the absorption modulation is equal to the atomic density modulation. In our case, the dimension of the cloud is larger than the depth of field of the imaging system, and therefore we expect a loss of contrast on the image. We calculated that, starting from a density modulation of 100% and considering the y dimension and the x dimension of the atomic cloud to be identical, the image will display 55% of absorption modulation. Note that we neglect the additional contrast decrease due to diffusion of free atoms during the flash detection phase. The average path of an atom during this phase can be roughly evaluated between 5 and 10 μm. The corrected density modulation is 54% and it has to be compared to the spatial variation of the depth of potential wells. For the beam configuration that we are considering and for a $4 \rightarrow 5$ transition, the adiabatic depth of the deepest wells is two times the depth of the shallowest ones (we are considering the most light-shifted state). If the atomic density were simply proportional to the depth of the wells, one could expect a density modulation of 33%. The difference with respect to the measured value of 54% confirms the nonlinear variation of the atomic density with the depth of the wells observed previously in numerical simulations [9]: the atoms fill preferentially the deepest potential wells.

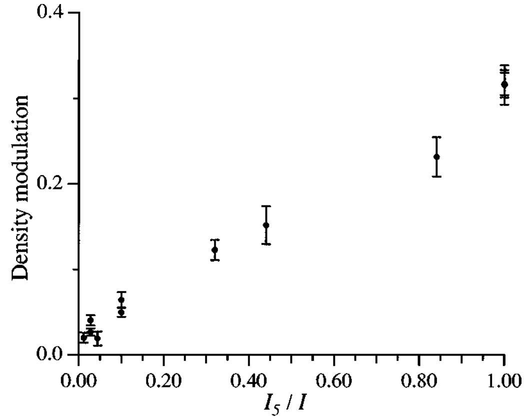

FIG. 4. Experimental variation of the density modulation depth as a function of the relative intensity I_5/I of the fifth beam. The data are obtained by analysis of shadow images like the one shown in Fig. 3.

Another interesting experiment can be done by attenuating the fifth beam. We illustrate in Fig. 4 the density modulation measured when the intensity of the fifth beam is varied from zero up to the intensity of the other lattice beams (I_5/I varies from 0 to 1). This variation of the density modulation can be related to the buildup of the quasiperiodic order measured previously by Bragg scattering [9]. The present behavior is very similar, and now this direct measurement needs no evaluation of the scattering efficiency of a single atom [7]. It is interesting to note that the density modulation observed in these images has a close connection with the Rayleigh stimulated scattering measured in pump-probe spectroscopy. Indeed, the Rayleigh component originates from the scattering of the pumps from the density grating induced by the probe [22]. In the present experiment, we have measured an uncorrected density modulation of 2% when $I_5/I = 0.03$ (in this situation, the modulation depth of the adiabatic potential is approximately 3%). For a degenerate excitation in pump-probe spectroscopy, density modulations of a few percent are thus expected, even with probes 30 times weaker than the lattice beams.

In conclusion, the direct observation of a superlattice clearly confirms that the atoms accumulate in the deepest wells of a nonperiodic optical lattice, as hitherto inferred only from indirect clues [8,9]. The superperiodic optical lattice that we studied is described by two different length scales: the potential-wells size (of the order of the optical wavelength λ) and the long-range depth modulation (tunable, just by varying an angle, in the 10–500-μm range). Our experiment clearly shows that the presence of local minima does not impede the atomic motion towards the deepest potential wells. Therefore, such kinds of superlattices could be used to increase the probability of finding two atoms in the same potential well. Up to now, we have only considered the static properties of this superlattice. In the near future, we plan to use it to study the diffusion of the atoms in the periodic four-beam lattice. For that, we shall need to modify the setup to be able to turn off rapidly the fifth beam. Recording a set of successive images after the extinction of this beam, we should be able to measure how the density modulation decreases. This measurement could be compared with the same kind of information obtained by the coherent transient method [23]. Alternatively, by changing the frequency of the fifth beam, we are able to observe how the density grating follows the intensity grating. A complete experiment would support the interpretation of the Rayleigh component of pump-probe transmission spectra in terms of diffraction on the density grating induced by the probe.

The authors wish to thank Claude Cohen-Tannoudji, Gilbert Grynberg, Jean-Yves Courtois, and Christophe Salomon for stimulating discussions. L.G. gratefully acknowledges support from the Collège de France. We are also grateful to E. Drean from Photonetics for lending us the 16-bit CCD camera. Laboratoire Kastler Brossel is ''Unité de Recherche de l'Ecole Normale Supérieure et de l'Université Pierre et Marie Curie, associée au CNRS.''

[1] For reviews on optical lattices, see P. S. Jessen and I. H. Deutsch, in *Advances in Atomic, Molecular, and Optical Physics 37*, edited by B. Bederson and H. Walther (Academic Press, Cambridge, 1996); W. D. Phillips, in *Coherent and Collective Interactions of Particles and Radiation Beams*, Proceedings of the International School of Physics Enrico Fermi, Course CXXXI, Varenna, 1996, edited by A. Aspect, W. Barletta, and R. Bonifacio (IOS Press, Amsterdam, 1996), p. 209; G. Grynberg and C. Triché, *ibid.*, p. 243; A. Hemmerich, M. Weidemüller, and T. W. Hänsch, *ibid.*, p. 583.

[2] F. Bloch, Z. Phys. **52**, 555 (1929).

[3] M. Ben Dahan *et al.*, Phys. Rev. Lett. **76**, 4508 (1996).

[4] P. Verkerk *et al.*, Phys. Rev. Lett. **68**, 3861 (1992).

[5] P. Jessen *et al.*, Phys. Rev. Lett. **69**, 49 (1992).

[6] G. Birkl *et al.*, Phys. Rev. Lett. **75**, 2823 (1995).

[7] M. Weidemüller *et al.*, Phys. Rev. Lett. **75**, 4583 (1995).

[8] L. Guidoni *et al.*, in *Trends in Optics and Photonics TOPS 7. Ultracold Atoms & Bose-Einstein Condensation*, edited by K. Burnett (Optical Society of America, Washington, DC, 1997), p. 77.

[9] L. Guidoni *et al.*, Phys. Rev. Lett. **79**, 3363 (1997).

[10] For a review on quasicrystals, see, for example, *Lectures on Quasicrystals*, edited by F. Hippert and D. Gratias (Les Editions de Physique, Paris, 1994).

[11] G. Grynberg *et al.*, Phys. Rev. Lett. **70**, 2249 (1993).

[12] For an overview of solid-state semiconductor superlattices, see, for example, G. Bastard, J. A. Brum, and R. Ferreira, in *Solid State Physics 44*, edited by H. Ehrenreich and D. Turnbull (Academic, San Diego, 1991), p. 229, and references therein.

[13] More precisely, the situation that we consider is very similar to the semiconductor superlattices in which the component concentrations vary continuously (''n-i-p-i'' crystals). See, for example, H. Döhler, IEEE J. Quantum Electron. **QE22**, 1682 (1986).

[14] E. L. Raab *et al.*, Phys. Rev. Lett. **59**, 2631 (1987); C. Monroe *et al.*, *ibid.* **65**, 1571 (1990).

[15] C. Cohen-Tannoudji, in *Fundamental Systems in Quantum Optics*, edited by J. Dalibard, J.-M. Raimond, and J. Zinn-Justin (Elsevier Science, Amsterdam, 1992).

[16] The resolution of our imaging system is deduced from the manufacturer specifications of the single optical elements (Melles Griot catalog 1997/1998).

[17] N. P. Bigelow and M. G. Prentiss, Phys. Rev. Lett. **65**, 29 (1990).

[18] A. Steane, M. Chowdhury, and C. J. Foot, J. Opt. Soc. Am. B **9**, 2142 (1992).

[19] T. T. Grove *et al.*, Phys. Rev. A **51**, R4325 (1995).

[20] D. Boiron and C. Salomon (private communication).

[21] M. Walhout *et al.*, Phys. Rev. Lett. **74**, 506 (1995).

[22] J.-Y. Courtois, in *Coherent and Collective Interactions of Particles and Radiation Beams* (Ref. [1]), p. 341.

[23] C. Triché *et al.*, in *Trends in Optics and Photonics TOPS 7. Ultracold Atoms & Bose-Einstein Condensation* (Ref. [8]), p. 82.